Journal of Experimental Botany, Vol. 70, No. 21 pp. 6447–6459, 2019
doi:10.1093/jxb/erz386 Advance Access Publication August 24, 2019
This paper is available online free of all access charges (see https://academic.oup.com/jxb/pages/openaccess for further details)

RESEARCH PAPER

Elevated CO_2 alleviates the negative impact of heat stress on wheat physiology but not on grain yield

Sachin G. Chavan[1,*], Remko A. Duursma[1], Michael Tausz[2,†] and Oula Ghannoum[1]

[1] ARC Centre of Excellence for Translational Photosynthesis, Hawkesbury Institute for the Environment, Western Sydney University, Locked Bag 1797 Penrith NSW 2751 Australia
[2] Department of Forest and Ecosystem Science, The University of Melbourne, 4 Water Street, Creswick, Vic. 3363, Australia

[†] Present address: School of Health Medical and Applied Sciences, CQ University, Queensland, Australia
* Correspondence: S.Chavan@westernsydney.edu.au

Received 16 May 2019; Editorial decision 15 August 2019; Accepted 6 September 2019

Editors: Robert Hancock, The James Hutton Institute, UK

Abstract

Hot days are becoming hotter and more frequent, threatening wheat yields worldwide. Developing wheat varieties ready for future climates calls for improved understanding of how elevated CO_2 (eCO_2) and heat stress (HS) interactively impact wheat yields. We grew a modern, high-yielding wheat cultivar (Scout) at ambient CO_2 (aCO_2, 419 µl l^{-1}) or eCO_2 (654 µl l^{-1}) in a glasshouse maintained at 22/15 °C (day/night). Half of the plants were exposed to HS (40/24 °C) for 5 d at anthesis. In non-HS plants, eCO_2 enhanced (+36%) CO_2 assimilation rates (A_{sat}) measured at growth CO_2 despite down-regulation of photosynthetic capacity. HS reduced A_{sat} (–42%) in aCO_2- but not in eCO_2-grown plants because eCO_2 protected photosynthesis by increasing ribulose bisphosphate regeneration capacity and reducing photochemical damage under HS. eCO_2 stimulated biomass (+35%) of all plants and grain yield (+30%) of non-HS plants only. Plant biomass initially decreased following HS but recovered at maturity due to late tillering. HS equally reduced grain yield (–40%) in aCO_2- and eCO_2-grown plants due to grain abortion and reduced grain filling. While eCO_2 mitigated the negative impacts of HS at anthesis on wheat photosynthesis and biomass, grain yield was reduced by HS in both CO_2 treatments.

Keywords: Climate change, elevated CO_2, grain yield, heat stress, photosynthetic acclimation, temperature response, wheat.

Introduction

Rising atmospheric CO_2 concentration is the primary cause of increasing global mean surface temperatures as well as increased frequency, duration, and intensity of heat waves. Heat stress (HS), defined as short-term temperature increases above the optimum range (Wahid *et al.*, 2007), and other climate extremes such as droughts threaten global crop productivity, including wheat (Asseng *et al.*, 2015). Wheat (*Triticum aestivum* L.) is the most widely grown crop (>218 Mha planted annually) in the world, the second most produced cereal globally (771 Mt in 2017) after maize (1134 Mt in 2017) (FAO, 2019), and a significant source of protein, providing ~20% of global calories for human consumption. Recent trends in climate and global crop production (Lobell *et al.*, 2011) raise pertinent questions about the readiness of current crop genotypes to cope with future climate extremes, and highlight the need to evaluate the performance of current commercial, high-yielding crop genotypes under elevated CO_2 (eCO_2) and HS conditions.

Several studies have investigated the response of wheat to eCO_2 (Kimball, 1983; Hocking and Meyer, 1991; Kimball *et al.*, 1995, 1999; Nie *et al.*, 1995; Hunsaker *et al.*, 1996,

2000; Miglietta *et al.*, 1996; Osborne *et al.*, 1998; Amthor, 2001). However, only a few studies have considered the interaction between eCO_2 and warming in wheat (Rawson, 1992; Delgado *et al.*, 1994; Morison and Lawlor, 1999; Jauregui *et al.*, 2015; Cai *et al.*, 2016), and less frequently included HS (Wang *et al.*, 2008, 2011; Shanmugam *et al.*, 2013; Fitzgerald *et al.*, 2016). Studies considering acute HS alone (Stone and Nicolas, 1994, 1996, 1998) or with eCO_2 focused mainly on biomass or yield and not the underlying physiological processes such as photosynthesis. Only a few studies have considered the interactive effects of eCO_2 and HS on wheat photosynthesis (Wang *et al.*, 2008, 2011; Shanmugam *et al.*, 2013; Macabuhay *et al.*, 2018). These studies emphasize the need to determine the impacts of HS application at the vegetative and the important reproductive stage.

The FACE (free-air CO_2 enrichment) study by Fitzgerald *et al.* (2016) in wheat relied on natural heat waves during the reproductive stage and highlighted the need for controlled-environment experiments in order to carefully investigate the interactive effects of eCO_2 and HS on wheat productivity. The only FACE study with wheat by Macabuhay *et al.* (2018) involved controlled heat stress along with eCO_2 and concluded that eCO_2 may moderate some effects of HS on wheat grain yield, but such effects strongly depend on seasonal conditions and timing of HS. The limited number of studies highlight the gap in our understanding of how processes underlying wheat yield respond to the interactive effects of eCO_2 and HS. Such understanding is important to identify potential adaptive traits for future breeding in order to stay abreast of climate change.

HS may cause irreversible effects on plant growth and development (Wahid *et al.*, 2007), and can inhibit both light and dark processes of photosynthesis via numerous mechanisms (Farooq *et al.*, 2011). For example, temperatures >45 °C can damage PSII (Berry and Bjorkman, 1980; Sage and Kubien, 2007). Plants may acclimate and acquire thermal tolerance to HS by activating stress response mechanisms and expressing heat shock proteins to repair HS damage (Pan *et al.*, 2018; Zhang *et al.*, 2018). Acquired thermotolerance is cost intensive and compromises plant productivity (Wahid *et al.*, 2007).

Elevated CO_2 reduces stomatal conductance and increases photosynthesis rates by stimulating carboxylation and suppressing oxygenation of Rubisco known as photorespiration (Ainsworth and Rogers, 2007; Leakey *et al.*, 2009). Photosynthesis responds transiently to an instantaneous increase in temperature but may acclimate in response to long-term exposures (>1 d) to high temperature (Yamasaki *et al.*, 2002). Above the thermal optimum (T_{opt}), high temperature reduces photosynthesis by increasing photorespiration and decreasing Rubisco activation (Eckardt and Portis, 1997). The maximal rate of RuBP carboxylation (V_{cmax}) responds positively to temperatures as high as 40 °C, but the maximal rate of ribulose bisphosphate (RuBP) regeneration or electron transport (J_{max}) generally decreases at lower temperatures in the range of 33 °C (Medlyn *et al.*, 2002). The relative effect of eCO_2 on net photosynthesis is greater at high temperatures due to suppression of photorespiration (Long, 1991). Elevated CO_2 may also increase the T_{opt} of photosynthesis (Borjigidai *et al.*, 2006; Alonso *et al.*, 2008; Ghannoum *et al.*, 2010). At eCO_2, the response of photosynthesis to temperature becomes increasingly limited by J_{max} and Rubisco activation (Sage and Kubien, 2007). Therefore, the T_{opt} of photosynthesis will reflect that of J_{max} in plants grown at eCO_2. Above T_{opt}, acclimation of photosynthesis to high temperatures is associated with increased electron transport and/or heat stabilty of Rubisco activase (Sage and Kubien, 2007). Hence, even though J_{max} decreases with short-term increases in temperature, prolonged exposure to high temperaure may trigger photosynthetic acclimation and increase J_{max}. Consequently, we predict that eCO_2 will increase the T_{opt} of photosynthesis, and mitigate negative effects of HS on photosynthesis via increased electron transport (Hypothesis 1).

The effects of HS on plant biomass and grain yield depend on the magnitude and duration of HS. HS at the vegetative stage reduces biomass and grain yield mainly by speeding up plant development and reducing the time available to capture resources, and by reducing photosynthetic rates (Lobell and Gourdji, 2012). At the flowering or anthesis stage, HS reduces grain number due to pollen abortion, while at the grain-filling stage, HS reduces grain weight by limiting assimilate translocation and shortening the grain-filling duration (Wahid *et al.*, 2007; Farooq *et al.*, 2011; Prasad and Djanaguiraman, 2014). Elevated CO_2 may alleviate the negative impact of HS on biomass and grain yield through stimulation of photosynthesis, improvement in plant water status due to reduced transpiration, and protection of the photosynthetic apparatus from HS damage. Furthermore, increased levels of sucrose and hexoses in plants grown at eCO_2 are associated with increased spike biomass and fertile florets (Dreccer *et al.*, 2014) and osmotic adjustment (Wahid *et al.*, 2007) which can improve HS tolerance (Shanmugam *et al.*, 2013). Taken together, we hypothesize that HS applied at anthesis will negatively impact plant biomass and grain yield less in eCO_2 than in ambient CO_2 (aCO_2) (Hypothesis 2).

The primary objective of this study was to test the performance of a current wheat champion genotype under future climate extremes. The chosen wheat cultivar, Scout, is a high yielding variety with very good grain quality and contains a putative high transpiration efficiency gene which can increase water use efficiency (https://www.pacificseeds.com.au/images/Icons/Products/Wheat/SNSWVICSA/ScoutVICSA.pdf). Considering the limitations of field conditions, we undertook our study under controlled environments to unravel the physiological underpinnings of the responses to eCO_2 and HS. Consequently, we grew wheat (cultivar Scout) plants in a glasshouse at current aCO_2 and future eCO_2, and exposed half of the plants to a 5 d HS at 50% anthesis (Zadoks scale DC65). We investigated the interactive effects of eCO_2 and HS on photosynthesis, biomass, and grain yield in Scout plants.

Materials and methods

Plant culture and treatments

The experiment was conducted in a glasshouse located at the Hawkesbury campus of Western Sydney University, Richmond, New South Wales. The commercial wheat cultivar Scout, which has a putative transpiration use efficiency gene (Condon *et al.*, 2004), was selected for the current

experiment. Seeds were sterilized using 1.5% $NaOCl_2$ for 1 min followed by incubation in the dark at 28 °C for 48 h in Petri plates. Sprouted seeds were planted in germination trays using seed raising and cutting mix (Scotts, Osmocote®) at ambient CO_2 (419 µl l^{-1}, day time average), temperature 22.3/14.8 °C (day/night average), relative humidity (RH; 62%, day time average), and natural light (see Supplementary Fig. S1a–e at *JXB* online). Day and night time averages were calculated from 10.00 h to 16.00 h and from 20.00 h to 06.00 h, respectively. Two-week-old seedlings were transplanted into individual cylindrical pots (15 cm diameter and 35 cm height) filled with sieved soil collected from the local site. Two glass house chambers were used for plant growth treatments, one with aCO_2 and the other with eCO_2. Each chamber had two bays with 50 plants in each bay. Fifty pots with one plant per pot were placed close to each other with a density of 24 plants m^{-2}. At the transplanting stage, pots were randomly distributed into aCO_2 and eCO_2 chambers. Transplanted plants were grown under the current aCO_2 (419 µl l^{-1}, daytime average) and eCO_2 (654 µl l^{-1}, day time average) with 62 % (day time average) RH, 22.3/14.8 °C (day/night average) growth temperature, and natural light (800 µmol m^{-2} s^{-1}, average daily maximum) (Supplementary Figs S1, S2). Half of the aCO_2- and eCO_2-grown plants were exposed to a 5 d HS treatment at 50% anthesis (13 weeks after planting, WAP). HS was applied by moving plants to a separate neighbouring chamber maintained at 40/24 °C (day/night average) air temperature and 71% (daytime average) RH during the 5 d HS treatment (Supplementary Figs S1a–e, S3). Plants were well watered throughout the experiment to separate HS and water stress effects. Thrive all-purpose fertilizer (Yates) was applied monthly throughout the experiment. To minimize chamber effects, pots were randomized regularly within and among the glasshouse chambers. Ten plants per treatment were used for physiological and biomass measurements.

Temperature response of leaf gas exchange at five leaf temperatures

The response of the light-saturated CO_2 assimilation rate (A_{sat}) to variations in substomatal CO_2 mole fraction (C_i) was measured at five leaf temperatures (15, 20, 25, 30, and 35 °C) in both aCO_2- and eCO_2-grown plants before HS. Saturating light of 1800 µmol m^{-2} s^{-1} photosynthetic photon flux density (PPFD) was used for measurements. Six plants per treatment were used to measure one A–C_i curve (see below for details) at each temperature. Plants were transferred into a growth cabinet (Sanyo) with temperature and light control to achieve the desired leaf temperature by controlling air temperatures. Leaf temperature sequence started at 25 °C decreasing to 15 °C and then increased up to 35 °C. Dark respiration (R_d) was measured by switching the light off for 20 min at the end of each temperature curve.

Single leaf gas exchange measurements

Instantaneous steady-state leaf gas exchange measurements were performed before (9 WAP), during (13 WAP), after (13 WAP), and at the recovery stage (17 WAP) of the HS cycle using a portable open gas exchange system (LI-6400XT, LI-COR, Lincoln, NE, USA, equipped with a leaf fluorometer). Measurements were performed at a PPFD of 1800 µmol m^{-2} s^{-1} with two CO_2 concentrations (400 µl l^{-1} and 650 µl l^{-1}) and two leaf temperatures (25 °C and 35 °C). Measuring plants at common 25 °C gives an idea about photosynthetic acclimation, while measuring plants at common 35 °C indicates the effects of HS relative to control plants. Plants were moved to a neighbouring growth chamber to achieve the desired leaf temperature.

Parameters measured were light-saturated assimilation rate (A_{sat}), stomatal conductance (g_s), the ratio of intercellular to ambient CO_2 (C_i/C_a), dark respiration (R_d), and maximum light use efficiency of PSII of dark- and light-adapted leaves (F_v/F_m and F_v'/F_m', respectively). These parameters were also measured in control plants before HS (13 WAP) and at the recovery stage (17 WAP) following HS. Photosynthetic down-regulation or acclimation was examined by comparing the measurements at common CO_2 (aCO_2- and eCO_2-grown plants measured at 400 µl CO_2 l^{-1}) and growth CO_2 (aCO_2-grown plants measured at 400 µl CO_2 l^{-1} and eCO_2-grown plants measured at 650 µl CO_2 l^{-1}). R_d was measured after a 15–20 min dark adaptation period. Photosynthetic water use efficiency (PWUE), also termed intrinsic water use efficiency, was calculated as A_{sat} (µmol m^{-2} s^{-1})/g_s (mol m^{-2} s^{-1}). The response of the A_{sat} to variations in C_i (A–C_i response curve) was measured at 17 WAP in eight steps of CO_2 concentrations (50, 100, 230, 330, 420, 650, 1200. and 1800 µl l^{-1}) at a leaf temperature of 25 °C. Measurements were taken around mid-day (from 10.00 h to 15.00 h) on attached fully expanded flag leaves (last leaves) of the main stems. Before each measurement, the leaf was allowed to stabilize for 10–20 min until it reached a steady state of CO_2 uptake and stomatal conductance. Ten replicate plants per treatment were measured.

Determination of Rubisco content

Following gas exchange measurements, leaf discs (0.5 cm^2) were collected using a cork borer from measured flag leaves, rapidly frozen in liquid nitrogen, and stored at –80 °C until analysed. Each leaf disc was extracted in 0.8 ml of ice-cold extraction buffer [50 mM EPPS–sodium hydroxide (pH 7.8), 5 mM DTT, 5 mM magnesium chloride, 1 mM EDTA, 10 µl of protease inhibitor cocktail (Sigma), and 1% (w/v) polyvinyl polypyrrolidone] using a 2 ml Tenbroeck glass homogenizer kept on ice. The extract was centrifuged at 15 000 rpm (21 130 rcf) for 1 min and the supernatant was used for the assay of Rubisco content. Samples were incubated in activation buffer [50 mM EPPS (pH 8.0), 10 mM $MgCl_2$, 2 mM EDTA, 20 mM $NaHCO_3$] for 15 min at room temperature. Rubisco content was estimated by the irreversible binding of [^{14}C]CABP (2-C-carboxyarabinitol 1,5-bisphosphate) to the fully carbamylated enzyme (Sharwood *et al.*, 2008).

Growth and biomass measurements

Plants were harvested at three time points: before HS (B), after recovery from HS (R), and at the final harvest after maturity (M). At each harvest, morphological parameters were measured and the biomass was harvested separately for roots, shoots, and leaves. Samples were dried for 48 h in the oven at 60 °C immediately after harvesting. Leaf area was measured before HS and at the recovery stage of HS using a leaf area meter (LI-3100A, LI-COR). Plant height, leaf number, tiller number, and spike (grain-bearing plant organ) number were also recorded. Leaf mass per area (LMA, g m^{-2}) was calculated as total leaf dry mass/total leaf area.

Mesophyll conductance and temperature response

Mesophyll conductance (g_m) was determined by concurrent gas exchange and stable carbon isotope measurements using a portable gas exchange system (LI-6400-XT, LI-COR) connected to a tunable diode laser (TDL) (TGA100, Campbell Scientific, UT, USA) for Scout grown at ambient aCO_2 partial pressures. A_{sat} and $^{13}CO_2/^{12}CO_2$ carbon isotope discrimination were measured 35 d after planting at five leaf temperatures (15, 20, 25, 30, and 35 °C) and saturating light (1500 µmol quanta m^{-2} s^{-1}). Leaf temperature sequence started at 25 °C decreasing to 15 °C and then increased up to 35 °C. Response of A_{sat} to variations in C_i was measured at each leaf temperature. R_d was measured by switching the light off for 20 min at the end of each temperature curve. Measurements were made inside a growth cabinet (Sanyo) to achieve the desired leaf temperature. The photosynthetic carbon isotope discrimination (Δ) to determine g_m was measured as follows (Evans *et al.*, 1986):

$$\Delta = \frac{1000\varepsilon(\delta^{13}C_{sam} - \delta^{13}C_{ref})}{1000 + \delta^{13}C_{sam} - \varepsilon(\delta^{13}C_{sam} - \delta^{13}C_{ref})}. \quad (1)$$

$$\text{Where, } \varepsilon = \frac{C_{ref}}{C_{ref} - C_{sam}}. \quad (2)$$

C_{ref} and C_{sam} are the CO_2 concentrations of dry air entering and exiting the leaf chamber, respectively, measured by the TDL. g_m was calculated using correction for ternary and second-order effects (Farquhar and Cernusak, 2012; Evans and Von Caemmerer, 2013) following the next expression:

$$g_m = \frac{\frac{1+t}{1-t}\left(b - a_i - \frac{eR_d}{A+R_d}\right)\frac{A}{C_a}}{(\Delta_i - \Delta_o - \Delta_e - \Delta_f)}. \quad (3)$$

Where, Δ_i is the fractionation that would occur if the g_m were infinite in the absence of any respiratory fractionation (e=0), Δ_o is observed fractionation, and Δ_e and Δ_f are fractionation of ^{13}C due to respiration and photorespiration, respectively (Evans and Von Caemmerer, 2013).

$$\Delta_i = \frac{1}{1-t}a'\frac{1}{(1-t)}((1+t)b - a')\frac{C_i}{C_a}. \quad (4)$$

$$\Delta_e = \frac{1+t}{1-t}\left(\frac{eR_d}{(A+R_d)C_a}(C_i - \Gamma*)\right). \quad (5)$$

$$\Delta_f = \frac{1+t}{1-t}\left(f\frac{\Gamma*}{C_a}\right). \quad (6)$$

$$\text{Where, } t = \frac{(1+a')E}{2g^t_{ac}}. \quad (7)$$

The constants used in the model were as follows: E denotes the transpiration rate; g^t_{ac} is total conductance to diffusion in the boundary layer (ab=2.9‰) and in air (a=4.4‰); a' is the combined fractionation of CO_2 across the boundary layer and stomata; net fractionation caused by RuBP and phosphoenolpyruvate (PEP) carboxylation (b=27.3‰) (Evans *et al.*, 1986); fractionation with respect to the average CO_2 composition associated with photorespiration (f=11.6‰) (Lanigan *et al.*, 2008); and we assumed null fractionation associated with mitochondrial respiration in light (e=0).

Statistical analysis and curve fitting

The full factorial experimental design included measurement of 10 plants per treatment for gas exchange and biomass determination. Data analyses and plotting were performed using R computer software (R Core Team, 2017). The effect of treatments and their interactions were analysed using Student's *t*-test and linear modelling with ANOVA. The homogeneity of variance was tested using Levene's test from the car package. Significance tests were performed with ANOVA and post-hoc Tukey test using the 'glht' function in the multcomp package designed for multiple comparisons. Other packages were also used, including (but not limited to) lubridate (for effective use of dates in plots), sciplot (for plotting), doby (for calculating means and SEs), and visreg (for plotting). The significance levels for ANOVA were, ⋆P<0.05, ⋆⋆P<0.01, and ⋆⋆⋆P<0.001. Coefficient means were ranked using post-hoc Tukey test.

The Farquhar–von Caemmerer–Berry (FvCB) photosynthesis model was fit to the A–C_i response curve or chloroplastic CO_2 mole fraction (C_c), which was estimated from the g_m measurements performed in a previous experiment as described above. g_m was measured in plants grown at aCO_2 and assumed similar for plants grown at eCO_2 due to the small effect of growth CO_2 on g_m (Singsaas *et al.*, 2004). We employed the plantecophys R package (Duursma, 2015), which uses the FvCB model to perform fits using measured g_m and R_d values along with recently reported values for K_c, energy of activation (E_a) for K_c, K_o, and Γ⋆ in wheat (Silva-Pérez *et al.*, 2017). Different temperatures values for K_c, K_o, and Γ⋆were determined using the Arrhenius equation as follows,

$$f(Tk) = k_{25}\cdot\exp\left[\frac{E_a\cdot(Tk-298)}{R\cdot 298\cdot Tk}\right]. \quad (8)$$

Where E_a is the activation energy (in J mol^{-1}) and k_{25} is the value of the parameter at 25 °C. R is the universal gas constant (8.314 J mol^{-1} K^{-1}), and Tk is the leaf temperature in K. The activation energy term E_a describes the exponential rate of rise of enzyme activity with the increase in temperature. Fitting the FvCB model using the plantecophys package resulted in estimates of maximal Rubisco carboxylation rate (V_{cmax}) and maximal electron transport rate (J_{max}). The temperature correction parameter ($T_{correct}$) was set to False while fitting A–C_i curves using the plantecophys package. Means of coefficients were calculated using summaryBy function (in the doBy package). Means of estimated V_{cmax} and J_{max} values at five leaf temperatures were then fit by Arrhenius and peaked functions, respectively (Medlyn *et al.*, 2002), using the non-linear least square (nls) function in R to determine energy of activation for V_{cmax} (E_aV) and J_{max} (E_aJ), and entropy (ΔSJ). Temperature responses of V_{cmax} and R_d means were fit using Arrhenius Equation 8. The temperature coefficient Q_{10}, a measure of the rate of change of a parameter as a consequence of increasing the temperature by 10 °C, was also determined for R_d using the following equation:

$$R_d = R_d25\cdot Q_{10}{}^{[(T-25)/10]} \quad (9)$$

A peaked function (Harley *et al.*, 1992) derived Arrhenius function was used to fit the temperature dependence of J_{max}, and is given by the following equation:

$$f(Tk) = k_{25}\cdot\exp\left[\frac{H_a\cdot(Tk-298)}{R\cdot 298\cdot Tk}\right]\left[\frac{1+\exp\left(\frac{298\cdot\Delta S - H_d}{298\cdot R}\right)}{1+\exp\left(\frac{Tk\cdot\Delta S - H_d}{Tk\cdot R}\right)}\right] \quad (10)$$

Where H_a is the activation energy and k_{25} is the J_{max} value at 25 °C, H_d is the deactivation energy, and S is the entropy term. H_d and ΔS together describe the rate of decrease in the function above the optimum. H_d was set to constant 200 kJ mol^{-1} to avoid overparameterization. The temperature optimum of J_{max} was derived from Equation 2 (Medlyn *et al.*, 2002) and written as follows:

$$T_{opt} = \frac{H_d}{\Delta S - R\cdot\ln\left[\frac{E_a}{(H_d - E_a)}\right]} \quad (11)$$

The temperature response of A_{sat} was fit using a simple parabola equation (Crous *et al.*, 2013) to determine the temperature optimum of photosynthesis:

$$A_{sat} = A_{opt} - b\cdot(T - T_{opt})^2 \quad (12)$$

where T is leaf temperature during measurement of A_{sat}, T_{opt} represents the temperature optimum, and A_{opt} is the corresponding A_{sat} at T_{opt}. Steady-state gas exchange parameters g_m, g_s, C_i, and the J_{max} to V_{cmax} ratio were fit using the nls function with the polynomial equation:

$$y + A + Bx + Cx^2 \quad (13)$$

Results

In non-HS plants, photosynthetic acclimation to eCO_2 was stronger at the vegetative stage, while eCO_2 stimulated photosynthesis at 25 °C at all growth stages

To assess photosynthetic acclimation due to eCO_2, non-HS plants were measured at the peak growth period (13 WAP) and after 50% anthesis (17 WAP). At 13 WAP, growth under eCO_2 reduced A_{sat} measured at common CO_2 at both 25 °C (–12%, P=0.004) (Fig. 1a; Table 1; and Supplementary Table S1) and 35 °C (–13.3%, P=0.01) (Table 1; Supplementary Table S1). At 13 WAP, eCO_2 enhanced A_{sat} of non-HS plants measured at growth CO_2, at both 25 °C (+25%, P=0.003) (Fig. 1a; Table 1; Supplementary Table S1) and 35 °C (+39%, P<0.001) (Table 1; Supplementary Table S1).

Relative to 13 WAP, A_{sat} decreased after 50% anthesis (17 WAP), but was not affected by eCO_2 in non-HS plants measured at common CO_2 and 25 °C or 35 °C (Fig. 1b, c; Table 1; Supplementary Table S1). When non-HS plants were measured during anthesis at growth CO_2, eCO_2 increased A_{sat} at 25 °C (+36%, P<0.001) but not at 35 °C (Fig. 1b , c; Table 1; Supplementary

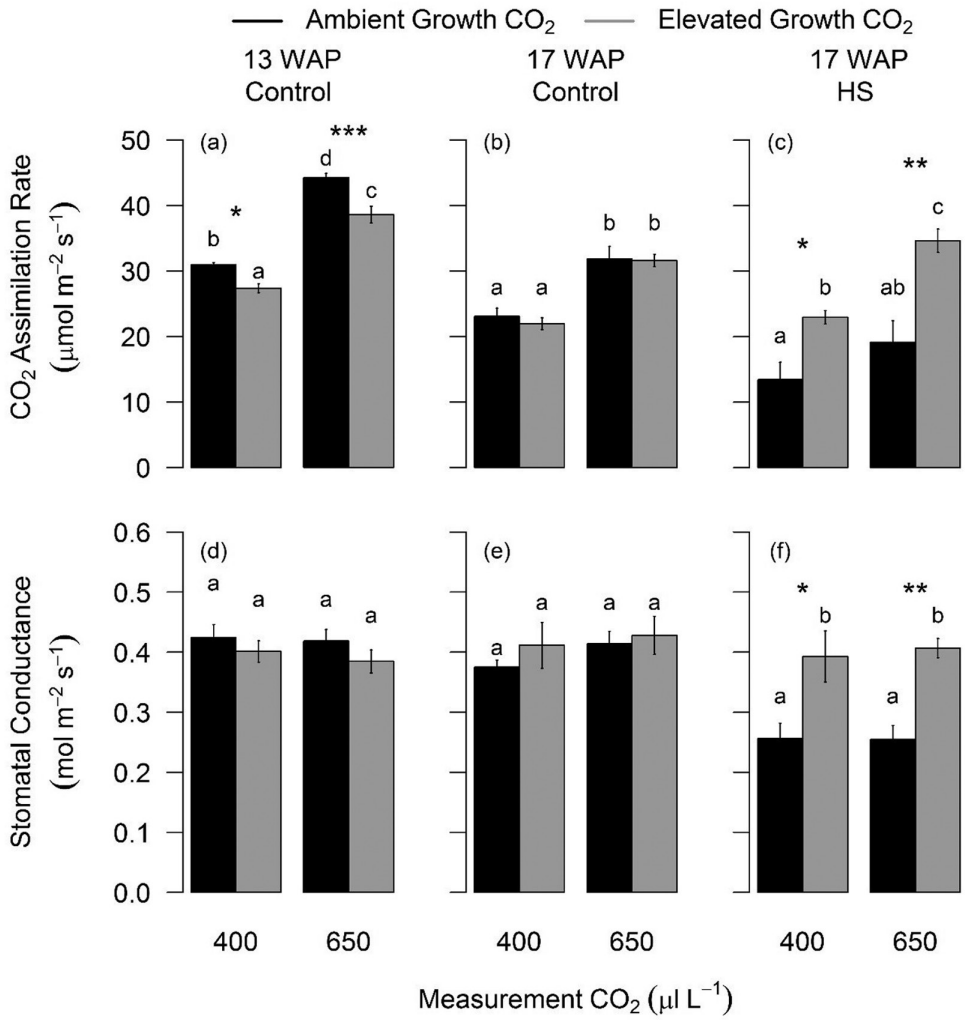

Fig. 1. Photosynthetic response of wheat cultivar Scout to eCO_2 measured 13 and 17 weeks after planting (WAP) at 25 °C leaf temperature and two CO_2 concentrations. Bar plot of means for light-saturated CO_2 assimilation rate (a, b, and c) and stomatal conductance (d, e, and f) calculated using two-way ANOVA. The error bars indicate the SE of the mean (n=9–10). Ambient and elevated CO_2-grown plants are depicted in black and grey, respectively. Grouping is based on measurement CO_2 (400 μl l^{-1} or 650 μl l^{-1}). Bars sharing the same letter in the individual panels are not significantly different according to Tukey's HSD test at the 5% level. Statistical significance levels (t-test) for eCO_2 effect are shown: *P<0.05; **P<0.01: ***P<0.001.

Table S1). eCO_2 had no significant effect on g_s of non-HS plants (Morison, 1998) measured 13 or 17 WAP at common or growth CO_2 (Fig. 1d–f; Table 1; Supplementary Table S1).

In non-HS plants, thermal responses of leaf gas exchange differed between aCO_2 and eCO_2 at higher temperatures

A–C_i curves were measured at five leaf temperatures to characterize the thermal photosynthetic responses of wheat plants grown at aCO_2 and eCO_2 (Fig. 2; Table 2; Supplementary Fig. S4). In non-HS, aCO_2- and eCO_2-grown Scout, A_{sat}, g_s, and C_i increased with temperature up to T_{opt} of ~23.5 °C and decreased more under eCO_2 relative to aCO_2 at higher temperatures. Relative to aCO_2, plants grown under eCO_2 had higher A_{sat} up to T_{opt} but similar A_{sat} at higher temperatures (Supplementary Fig. S4a). R_d increased with temperature under both aCO_2 and eCO_2; however, the rate of increase was slower at higher temperatures under eCO_2, resulting in lower R_d under eCO_2 relative to aCO_2 at 30°C and 35 °C. Nevertheless, energy of activation (E_aR) and the Q_{10} coefficient (rate of change due to an increase of temperature by 10 °C) of R_d were similar under aCO_2 and eCO_2 (Table 2; Supplementary Fig. S4b).

V_{cmax} and J_{max} were calculated by fitting the response of A_{sat} to variations in C_c (A–C_c response curve) using measured R_d and g_m. g_m increased up to 25 °C and remained relatively unchanged at higher temperatures (Supplementary Table S3). Within the range of measured leaf temperatures, V_{cmax} increased with leaf temperature, while J_{max} increased up to a T_{opt} of 28 °C and decreased thereafter. V_{cmax} and J_{max} decreased with eCO_2 at the two highest temperatures (Fig. 2). The J_{max}/V_{cmax} ratio was higher under eCO_2 relative to aCO_2 at lower temperatures and decreased with leaf temperature under aCO_2 or eCO_2 (eventually being similar at 35 °C) (Fig. 2). Despite variations in the temperature response, the overall fitted parameters were mostly similar in plants grown at aCO_2 or eCO_2, except for A_{opt} which was higher under eCO_2 (Table 2). There was no significant difference in V_{cmax} at 25 °C, J_{max} at 25 °C, *in vitro* measured Rubisco sites, or their activation energy under aCO_2 or eCO_2 (Fig. 2; Table 2).

Table 1. *Summary of statistics for gas exchange parameters*

Parameter (mean plant^{-1})	Measurement		13 WAP	17 WAP		
	Temperature °C	CO_2 (µl l^{-1})	Main effects	Main effects		Interaction
			CO_2	CO_2	HS	CO_2×HS
A (µmol m^{-2} s^{-1})	25	400	**	*	*	**
		650	**	**	*	**
	35	400	**	NS	NS	*
		650	**	NS	NS	*
R_d (µmol m^{-2} s^{-1})	25	400	NS	NS	NS	NS
	35	400	*			
g_s (mol m^{-2} s^{-1})	25	400	NS	*	*	NS
		650	NS	**	**	*
	35	400	NS	NS	NS	NS
		650	NS	NS	NS	NS
PWUE (A/g_s)	25	400	NS	NS	NS	NS
		650	NS	NS	NS	NS
	35	400	NS	NS	*	*
		650	NS	NS	NS	NS
F_v/F_m	25	400	NS	*	NS	NS
F_v'/F_m'	25	400	NS	**	**	*
A (µmol m^{-2} s^{-1})	25	Growth CO_2	**	***	NS	**
	35		***	**	NS	*
R_d (µmol m^{-2}s^{-1})	25		***			
	35		*			
g_s (mol m^{-2} s^{-1})	25		NS	***	**	*
	35		NS	NS	NS	NS
PWUE (A/g_s)	25		***	***	NS	*
	35		**	***	NS	NS

Summary of statistical analysis using two-way ANOVA for the effects of elevated CO_2 and heat stress (HS) on leaf gas exchange parameters measured at 13 and 17 weeks after planting (WAP). HS plants were measured at the recovery stage (n=9–10). Significance levels are **P<0.001; ** P <0.01; * P <0.05; NS, P>0.05.

Photosynthesis and PSII efficiency decreased during HS at both CO_2 treatments but recovered only under eCO_2

In this study, we successfully implemented a 5 d HS cycle at 50% anthesis as evidenced by the higher leaf temperature of the HS relative to the control plants (Supplementary Fig. S1f). Overall, HS reduced photosynthesis and was more damaging in aCO_2 than in eCO_2 plants (Fig. 4; Supplementary Table S1). Before HS (15 WAP), eCO_2 increased both A_{sat} (+43%, P<0.001) and g_s (+20%, P=0.032) measured at growth CO_2. HS reduced A_{sat} measured during and after HS in both CO_2 treatments. HS increased g_s measured during HS and reduced g_s after HS. One week after HS, both A_{sat} and g_s had completely recovered in eCO_2-grown plants but not in aCO_2-grown plants, which showed significant reductions in A_{sat} (–42%, P=0.017) and g_s (–32%, P=0.006) (Fig. 4a, c; Table 1; Supplementary Table S1).

The lasting negative effect of HS on photosynthesis at the recovery stage was associated with reduced V_{cmax} (–53%, P=0.002) in aCO_2- but not in eCO_2-grown plants. Conversely, the photosynthetic recovery after HS was associated with increased J_{max} (+37%, P=0.001) in eCO_2- but not in aCO_2-grown plants (Fig. 3d). Interestingly, HS significantly increased the J_{max}/V_{cmax} ratio in both aCO_2- and eCO_2-grown plants, but the ratio was not affected by growth CO_2.

Chlorophyll fluorescence measurements confirmed the persistent HS damage to photosynthesis in aCO_2- relative to eCO_2-grown plants. HS reduced light-adapted F_v'/F_m' measured after and at the recovery stage of HS in aCO_2- (–29%, P=0.019) but not in eCO_2-grown plants (Fig. 4d). HS reduced dark-adapted F_v/F_m in aCO_2- more than in eCO_2-grown plants; and F_v/F_m failed to recover in aCO_2 plants after HS (Fig. 4b).

At maturity, total plant biomass, but not grain yield, recovered from HS in both CO_2 treatments

Elevated CO_2 stimulated growth rate, biomass, and grain yield. A faster growth rate was evident from the larger number of ears (+127%, P<0.001) in eCO_2- relative to aCO_2-grown plants harvested 13 WAP (before HS) (Fig. 5). Elevated CO_2 significantly stimulated the total biomass harvested throughout the growing period (Fig. 5; Table 3; Supplementary Table S2). Total biomass stimulation was contributed by the overall increase in root, stem, and leaf biomass along with an increase in leaf area, leaf number, tiller number, and spike number (Table 3; Supplementary Table S2). At the final harvest, eCO_2-grown plants had 35% (P<0.001) more biomass and 30% higher grain yield (P=0.001) than aCO_2-grown plants under control conditions (Fig. 5; Table 3; Supplementary Table S2). The increase in grain yield of control plants under eCO_2 was due to an increased number of tillers and consequently ears (+22%, P<0.001), while the main shoot grain yield was not stimulated (Supplementary Table S2).

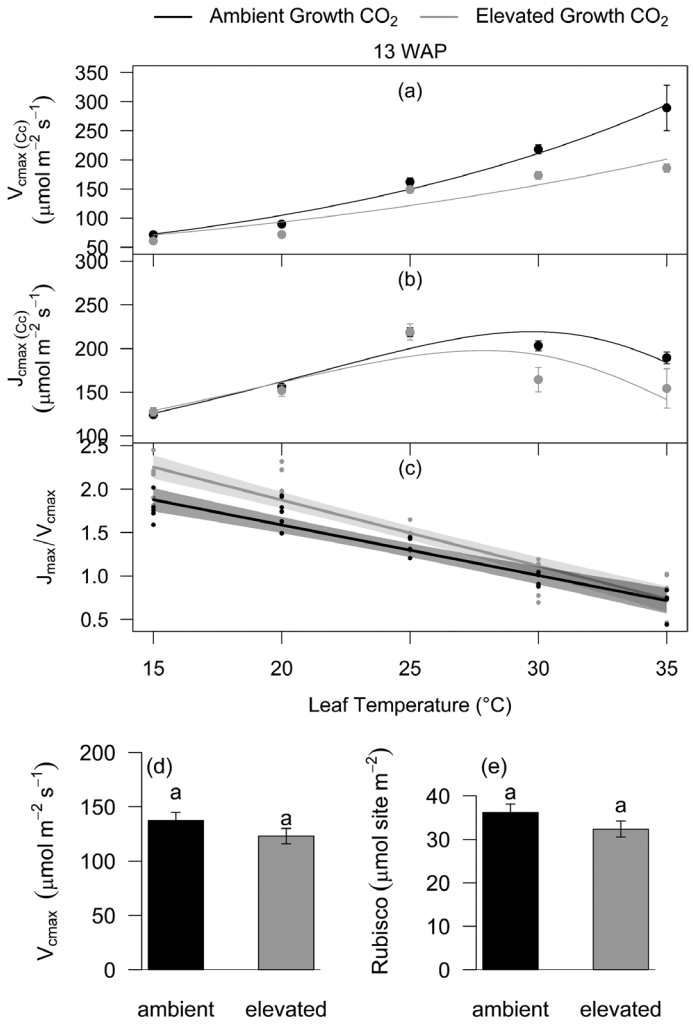

Fig. 2. *In vivo* Rubisco properties and temperature response of V_{cmax} and J_{max} measured 13 weeks after planting (WAP). Maximum velocity of carboxylation, V_{cmax} (a), maximum velocity of RuBP regeneration, J_{max} (b), and J_{max}/V_{cmax} ratio (c) determined using the response of CO_2 assimilation to variation in chloroplastic CO_2 (C_c) at five leaf temperatures (15, 20, 25, 30, and 35 °C) in wheat cultivar Scout (n=6). The ratio of J_{max}/V_{cmax} (c) is plotted using the visreg package in R. Regression lines are means with 95% confidence intervals. The lower panel is a bar plot showing *in vivo* V_{cmax} at 25 °C (n=6) (d) and Rubisco sites (n=5) (e) measured in flag leaf discs harvested at the same time point. For (a), (c), and (d), values are means ±SE. Ambient and elevated CO_2-grown plants are shown in black and grey, respectively.

Table 2. *Summary of modelled parameters for temperature response of photosynthesis*

Parameter	Constant	Ambient growth CO_2	Elevated growth CO_2
A_{sat} (µmol m^{-2} s^{-1})	T_{opt} (°C)	23.7±1.1 a	23.4±1.3 a
	A_{opt}	25.5±1.3 a	30.9±2.7 b
V_{cmax} (µmol m^{-2} s^{-1})	V_{cmax} at 25 °C	149±6 a	121±12 a
	E_aV (kJ mol^{-1})	51±4 a	38±10 a
J_{max} (µmol m^{-2} s^{-1})	J_{max} at 25 °C	200±12 a	190±22 a
	T_{opt} (°C)	29.5±0.7 a	27.5±0.9 a
	J_{max} at T_{opt}	233±6	210±11 a
	E_aJ (kJ mol^{-1})	37±11 a	34±22 a
	ΔSJ (J mol^{-1} K^{-1})	648±5 a	651±8 a
	H_d (kJ mol^{-1})	200	
R_d (µmol m^{-2} s^{-1})	R_d at 25 °C	2.4±0.1 a	2.2±0.1 a
	E_aR (kJ mol^{-1})	41±3 a	31±6 a
	Q_{10}	1.73±0.07 a	1.50±0.13 a

Summary of coefficients derived using non-linear least square fitting of CO_2 assimilation rates, maximal rate of carboxylation (V_{cmax}), and maximal rate of RuBP regeneration (J_{max}) determined using A–C_i response curves and dark respiration measured at five leaf temperatures (15, 20, 25, 30, and 35 °C). Values are means ±SEs. Derived parameters include temperature optima (T_{opt}) of photosynthesis (A_{opt}); activation energy for carboxylation (E_aV); activation energy (E_aJ), entropy term (ΔSJ), and T_{opt} and corresponding value for J_{max} with deactivation energy (H_d) assumed constant; and activation energy (E_aR) and temperature coefficient (Q_{10}) for dark respiration. Letters indicate significance of variation in means (n=6)

HS reduced the biomass of aCO_2 plants (–30%, P<0.001) more than eCO_2 plants (–10%, P=0.09) harvested at 17 WAP following the HS (Fig. 5; Supplementary Table S2). By the final harvest, HS plants recovered and had similar biomass relative to control plants grown under both aCO_2 and eCO_2. This recovery in biomass was driven by the HS-induced stimulation of additional late tillers and consequently new ears (Fig. 5).

Despite the recovery in biomass, the grain yield was similarly reduced by HS in both aCO_2- (–38%, P<0.001) and eCO_2- (–41%, P<0.001) grown plants due to grain abortion in old ears and insufficient grain filling in new ears (Fig. 6a, b; Supplementary Table S2). HS reduced grain yield of tillers (–77%, P<0.001) more than the main shoot (–45%, P<0.001), which developed earlier. In addition, HS reduced grain yield of tillers in plants grown at aCO_2 (–71 % P<0.001) less than in those grown at eCO_2 (–81%, P<0.001) due to their higher tiller number (Fig. 6c, d). This phenomenon is well recognized as growth stimulation at eCO_2 may limit grain yield due to trade-off between vegetative and reproductive components, including grains (Dias de Oliveira *et al.*, 2015). HS caused grain abortion, leading to empty ears without grains, or damaged and shrunken grains (Supplementary Fig. S5) evident from the reduction in grain per spike (–53%, P<0.001) and average grain weight (–25%, P<0.001) under both CO_2 treatments.

Discussion

Although field experiments are crucial to understand plant- and canopy-level responses to the environment, mechanistic and interactive analysis of climate change variables such as eCO_2 and temperature remains challenging in the field. In this study, we investigated the interactive effects of eCO_2 and HS on photosynthesis, biomass, and grain yield of Scout, a high-yielding modern wheat cultivar, under controlled environments. Wheat was grown at ambient or elevated CO_2 and exposed to a 5 d HS at 50% anthesis. eCO_2 stimulated photosynthesis, biomass, and grain yield, while HS reduced photosynthetic rates under aCO_2 and eCO_2. eCO_2 improved the recovery of photosynthesis and biomass following HS, but the HS-induced reduction in grain yield was similar under both CO_2 treatments due to grain abortion and inadequate grain filling. Our study demonstrated the interactive effects between eCO_2 and HS, providing insights into the mechanisms underlying the interactions, and identified a major discrepancy between the response of wheat photosynthesis and biomass versus grain yield to eCO_2×HS.

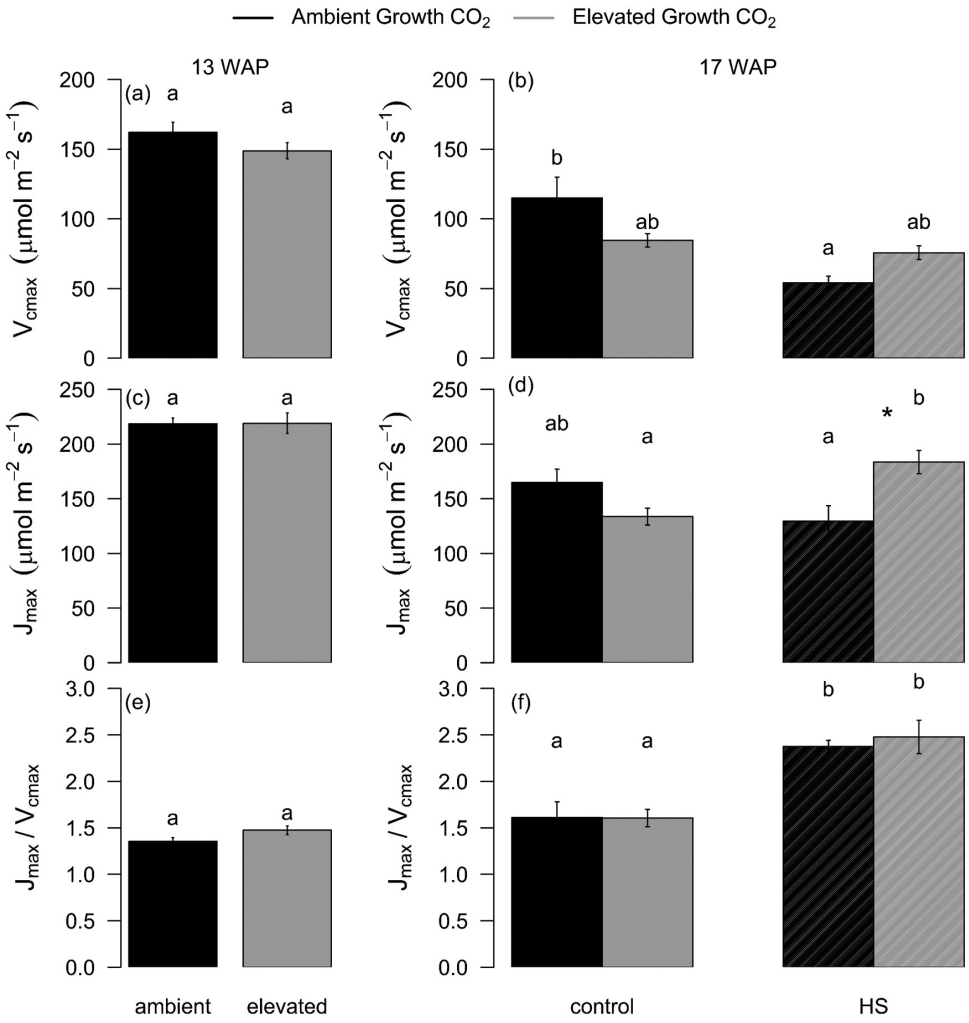

Fig. 3. Response of V_{cmax} and J_{max} to growth at eCO_2 and heat stress (HS) measured 13 and 17 weeks after planting (WAP) at the recovery stage of the HS cycle. Bar plot of means ±SE for V_{cmax} (a and b), J_{max} (c and d), and V_{cmax}/J_{max} (e and f) using two-way ANOVA. Leaf gas exchange was measured at 25 °C in ambient (black) and elevated (grey) CO_2-grown plants exposed (HS) or not exposed (Control) to a 5 d HS. Bars sharing the same letter in the individual panels are not significantly different according to Tukey's HSD test at the 5% level. The error bars indicate the SE of the mean (n=9–10). Statistical significance levels (t-test) for eCO_2 effect are shown: *P<0.05; **P<0.01: ***P<0.001.

The novelty of this study is in linking photosynthesis, biomass, and grain yield responses to the interactive effects of future climate variables. Our results and modelled parameters will be useful in developing a mechanistic modelling approach based on photosynthesis and parametrization of crop models that can predict yield under future extreme climate. Our results suggest that grain filling and translocation to the grain at high temperature are key weaknesses in modern high-yielding wheat varieties. Moreover, plastic tillering in response to eCO_2 and HS adversely impacted the final grain yield. These traits should be prioritized in current breeding programmes to sustain staple food production under future climate extremes.

Elevated CO_2 reduced photosynthetic electron transport capacity at high temperature

Elevated CO_2 modulates the instantaneous temperature response of photosynthesis (Sage and Kubien, 2007; Ghannoum *et al.*, 2010). Growth at eCO_2 slowed down the rate of increase in V_{cmax} and accentuated the decrease in J_{max} above T_{opt} in Scout (Fig. 2c), possibly due to reduced Rubisco activation and limitation in electron transport capacity at high temperature and eCO_2 (Sage and Kubien, 2007). Contrary to our hypothesis that eCO_2 will increase T_{opt} (Long, 1991), photosynthetic T_{opt} was similar under aCO_2 and eCO_2 (Table 2). Lower V_{cmax} and J_{max} at higher temperatures may have prevented the increase in T_{opt} under eCO_2, because the temperature dependence of J_{max} determines the shift of optimal temperature of photosynthesis at eCO_2 (Hikosaka *et al.*, 2006). Our results are consistent with a previous study by Alonso *et al.* (2008) where they found decreased V_{cmax} under eCO_2. In other wheat studies, eCO_2 increased V_{cmax} and J_{max} at supraoptimal temperatures, and reduced J_{max} at suboptimal temperatures (Alonso *et al.*, 2009). The discrepant V_{cmax} and J_{max} responses to our studies could be due to an unusual increase in V_{cmax} under eCO_2 observed in the study by Alonso *et al.* (2009). Modelled

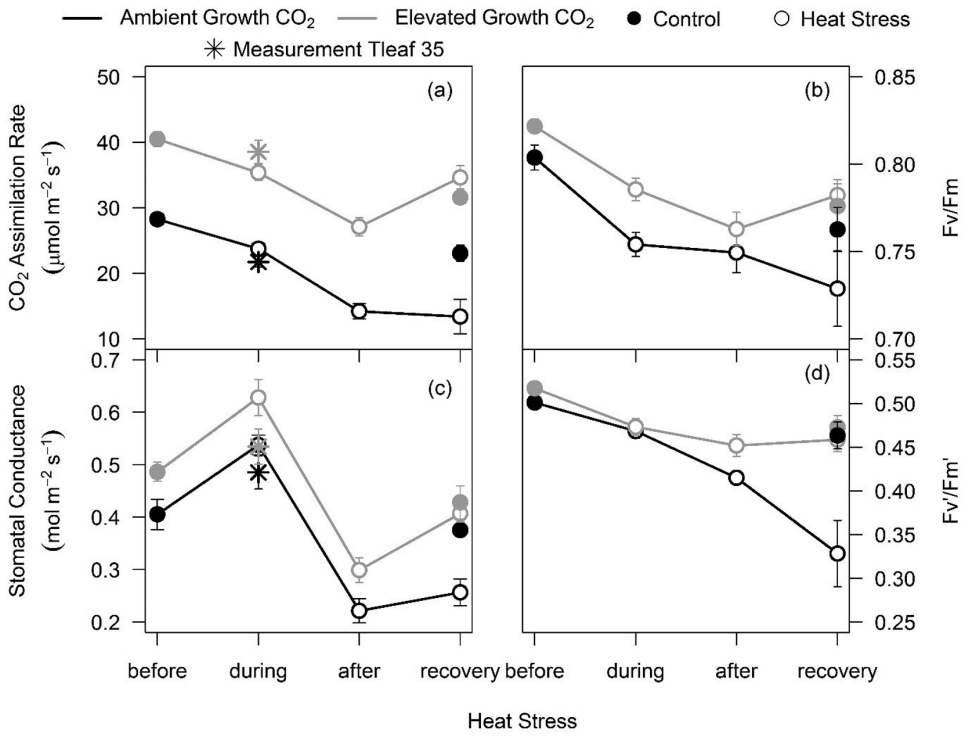

Fig. 4. Photosynthesis and chlorophyll fluorescence response of aCO_2- and eCO_2-grown wheat cv. Scout measured before, during, after, and at the recovery stage of the heat stress cycle. CO_2 assimilation rates (a), of the F_v/F_m ratio in dark-adapted leaves (b), stomatal conductance (c), and of the F_v'/F_m' ratio in light-adapted leaves (d) measured at growth CO_2 (aCO_2-grown plants measured at 400 µl l^{-1} and eCO_2-grown plants measured at 650 µl l^{-1}). Values are means ±SE (n=9–10). Ambient and elevated CO_2-grown plants are depicted in black and grey, respectively. Filled and open circles represent control and heat-stressed plants, respectively. The circle and star symbols depict CO_2 assimilation rates measured at 25 °C and 35 °C, respectively.

values of V_{cmax} at 25 °C (150 µmol m^{-2} s^{-1} and 121 µmol m^{-2} s^{-1} at aCO_2 and eCO_2, respectively) are similar to *in vitro* (137 µmol m^{-2} s^{-1} and 123 µmol m^{-2} s^{-1} at aCO_2 and eCO_2, respectively) values measured in the current study and previously reported in wheat (117 µmol m^{-2} s^{-1}) by Silva-Pérez *et al.* (2017). Modelled values of E_aV (51 kJ and 38 kJ at aCO_2 and eCO_2, respectively) were lower than E_aV (63 kJ) reported in the wheat study by Silva-Pérez *et al.* (2017).

Elevated CO_2 protected wheat photosynthesis by stimulating electron transport potential following HS

Generally, HS reduces net photosynthetic rates in wheat (Wang *et al.*, 2008), while the extent of the response depends on the cultivar (Sharma *et al.*, 2014). However, acclimation to long-term eCO_2 can modulate the photosynthetic responses to HS during the vegetative or anthesis stage (Wahid *et al.*, 2007). In Scout, photosynthetic rates recovered following HS under eCO_2 but not under aCO_2 (Fig. 4a), indicating that HS transiently reduced photosynthesis without eliciting permanent damage to the photosynthetic apparatus of eCO_2-grown plants. The recovery of photosynthesis under eCO_2 was associated with the recovery of the electron transport rate (Fig. 4d) and photochemical efficiency (Fig. 4a), maintenance of V_{cmax} (Fig. 3b), and increased J_{max} (Fig. 3d) relative to non-HS, eCO_2-grown plants, thus validating our hypothesis that eCO_2 will protect photosynthesis via increased electron transport. Higher J_{max} may have protected the photosynthetic apparatus from HS damage by increasing electron sinks, and hence photochemical quenching (Sage and Kubien, 2007). Higher J_{max} is also associated with higher Rubisco activation (Perdomo *et al.*, 2017), which may have helped recovery of photosynthesis under eCO_2.

In contrast, aCO_2-grown Scout suffered permanent loss of photosynthesis and photochemical efficiency (F_v/F_m) after HS. Reduced F_v/F_m is a sign of stress (Sharkova, 2001; Haque *et al.*, 2014) and indicates lower quantum efficiency of PSII (Baker, 2008). Damage to the photosynthetic apparatus was also evident from the reduction in V_{cmax} at aCO_2 (Fig. 3b), although J_{max} was not affected by HS (Fig. 3d). Consequently, the J_{max}/V_{cmax} ratio was equally increased by HS in both CO_2 treatments, suggesting increased resource allocation to RuBP regeneration or electron transport (Hikosaka *et al.*, 2006) in response to HS irrespective of growth CO_2. An enhanced J_{max}/V_{cmax} ratio by exposure to HS may potentially play a role in avoiding photoinhibition (Walker *et al.*, 2014).

In line with our results, photosynthesis and F_v/F_m were inhibited by HS (3 d at 40 °C) applied after anthesis in two wheat cultivars grown at aCO_2 but not at eCO_2 (Shanmugam *et al.*, 2013). Protection from HS damage of photosynthesis as a result of improved photochemical quenching or electron transport appears to be a universal mechanism in crops exposed to eCO_2. In tomato, HS (42 °C) reduced A_{sat} (–57%), V_{cmax}, and J_{max} (–45%) under aCO_2, while eCO_2 increased A_{sat} (+96%), V_{cmax}, and J_{max} after 24 h of recovery from HS (Pan *et al.*, 2018). In Arabidopsis, photosynthesis and chlorophyll fluorescence were less inhibited by HS (38 °C) in eCO_2 than in aCO_2 8 d after recovery (Zinta *et al.*, 2014). The study

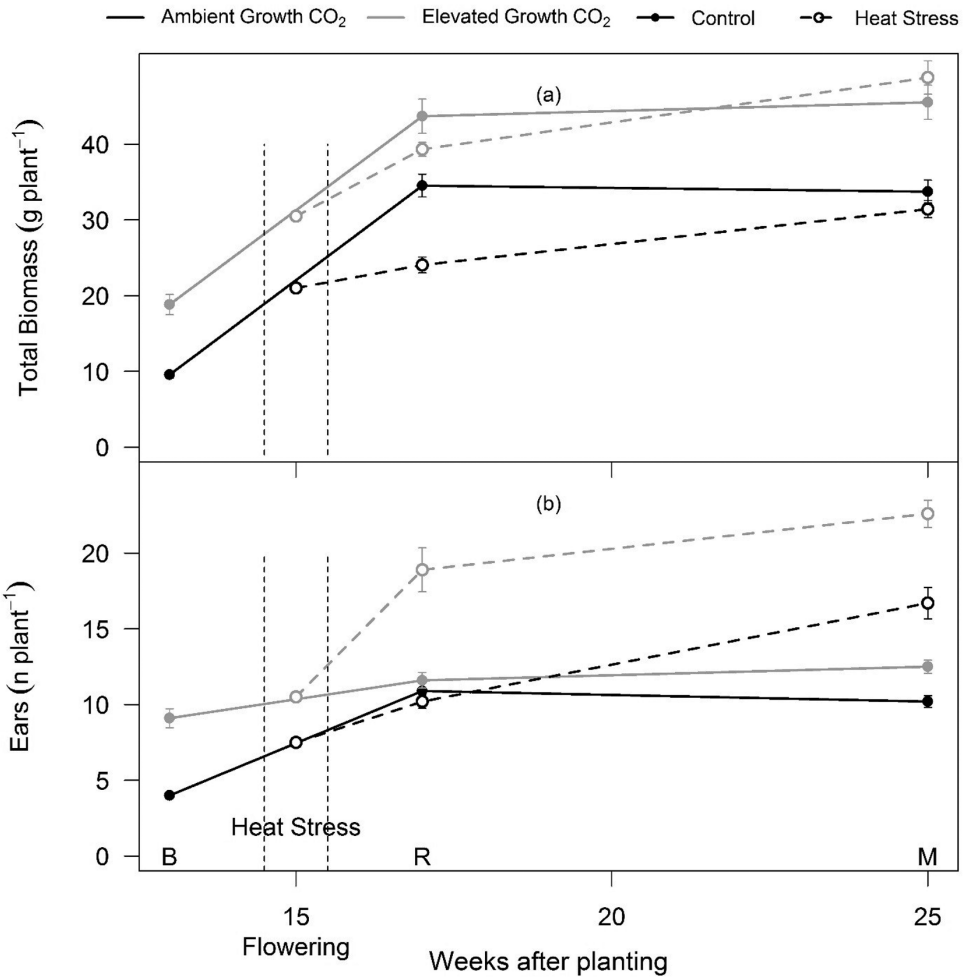

Fig. 5. Response of biomass and ears (or tillers) to eCO_2 and HS across the life cycle of wheat cv. Scout. Response of total biomass (a) and spike number (b) to eCO_2 and HS at three time points; before HS (B), after recovery from HS (R), and at the final harvest after maturity (M). Ambient and elevated CO_2-grown plants are depicted in black and grey, respectively. Solid and dotted lines represent control and heat-stressed plants, respectively. Filled and open circles represent control and heat-stressed plants, respectively. Vertical black dotted lines show the timing of HS. Symbols are means per plant ±SE (n=9–10).

concluded that eCO_2 mitigated HS stress impacts through up-regulation of antioxidant defence metabolism and reduced photorespiration, resulting in lowered oxidative pressure (Zinta *et al.*, 2014). In other studies investigating the interactive effects of eCO_2 and HS (reviewed by Wang *et al.*, 2011), eCO_2 enhanced the thermal tolerance of photosynthesis in both cool- and warm-season species, indicating that the mitigating effects of CO_2 were independent of the plant habitat (Hogan *et al.*, 1991; Wang *et al.*, 2008).

Following HS, plant biomass recovered in all plants due to late tillering, while grain yield declined even under eCO_2

Despite the initial negative impacts of HS on plant growth in Scout, total plant biomass recovered at maturity, and this was associated with positive source (photosynthesis) and sink (tiller) responses. As discussed earlier, HS caused irreversible photosynthetic damage at aCO_2, while growth at eCO_2 mitigated the negative impact of HS on photosynthesis. Moreover, the biomass of HS plants recovered under both CO_2 treatments due to late tiller and ear development (Bányai *et al.*, 2014). When grain development is stalled under certain conditions (e.g. HS), the crop develops new grains by producing additional late tillers. This is considered a non-harmful acclimation response to HS which creates additional sinks. Hence, grain abortion due to HS was compensated by the production of additional late tillers contributing to the recovery in biomass at the final harvest. An equal decrease in biomass under aCO_2 and eCO_2 following exposure to HS has been reported in a study using the C_3 crop *Sinapis alba* (white mustard), which also concluded that interactive effects of CO_2 and HS depend on species, magnitude of HS, and growth conditions (Coleman *et al.*, 1991). In cases where HS causes persistent reduction in biomass at aCO_2, eCO_2 often alleviates the negative impacts of HS (Zinta *et al.*, 2014). It is worth noting that the development of additional late ears and tillers following HS is expected to increase sinks for the translocation of assimilates. Greater sink strength may partly explain photosynthetic recovery in HS plants (Paul and Foyer, 2001). However, photosynthesis recovered in eCO_2 plants only, while late tillering was observed under both CO_2 treatments. Similarly, in wheat grown using growth chambers and exposed to moderate HS (32 °C) after anthesis, grain yield decreased under both ambient and elevated CO_2 (Zhang *et al.*, 2018). Althogh Scout biomass recovered in all plants exposed to HS, grain yield was equally

Table 3. *Summary of statistics for plant dry mass (DM) and morphological parameters*

Time point	Parameter (mean per plant)	Main effects		Interaction
		CO_2	HS	CO_2×HS
13 WAP (T1)	Tiller number	**		
	Leaf number	***		
	Leaf area (cm^2)	***		
	Ear number	***		
	Ear DM (g)	***		
	Leaf DM (g)	***		
	Stem DM (g)	***		
	Roots DM (g)	NS		
	Shoot DM (g)	***		
	Total DM (g)	***		
17 WAP (T2)	Tiller number	***	***	***
	Leaf number	***	***	***
	Leaf area (cm^2)	***	NS	**
	Ear number	***	***	***
	Ear DM (g)	***	***	NS
	Leaf DM (g)	***	***	***
	Stem DM (g)	***	***	***
	Roots DM (g)	***	**	*
	Shoot DM (g)	***	***	NS
	Total DM (g)	***	***	NS
25 WAP (T3)	Ear number	***	***	*
	Ear DM (g)	***	***	NS
	Roots DM (g)	NS	***	NS
	Shoot DM (g)	***	***	**
	Total DM (g)	***	NS	NS
	Main stem grain yield (g)	NS	***	NS
	Grain yield (g)	***	***	NS
	Grain number	**	***	NS
	Grains per ear	NS	***	NS
	Grain size (mg per grain)	**	***	NS
	Harvest index	**	***	*

Summary of statistical analysis using two-way ANOVA for the effects of elevated CO_2 and heat stress (HS) on biomass and morphological parameters for plants harvested at various time points (n=9–10). Significance levels are *** P <0.001; **P<0.01; *P<0.05; NS, P>0.05

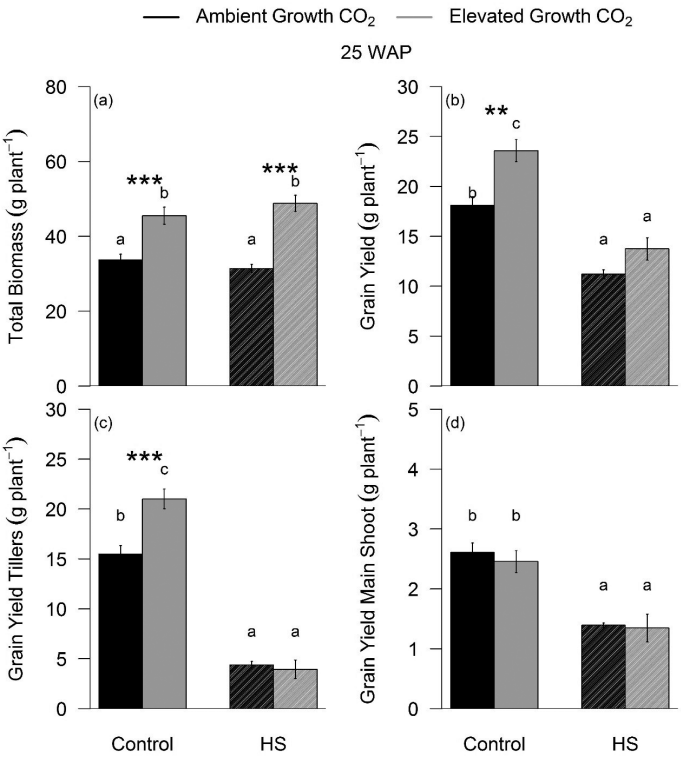

Fig. 6 Response of plant total biomass and grain yield to elevated CO_2 and heat stress (HS) at the final harvest. Bar plot of means ±SE for total biomass (a), grain yield (b), grain yield of tillers (c), and grain yield of the main shoot (d) using two-way ANOVA measured in ambient (black) and elevated (grey) CO_2-grown plants exposed (HS) or not exposed (Control) to a 5 d HS. Bars sharing the same letter in the individual panels are not significantly different according to Tukey's HSD test at the 5% level. Values are means ±SE (n=9–10). Statistical significance levels (t-test) for eCO_2 effect are shown: *P<0.05; **P<0.01: ***P<0.001.

reduced in both CO_2 treatments due to grain abortion in the old ears and insufficient time for grain filling in the new ears. In response to HS, some ears had completely lost grains, and ears with developing grains could not fill, leading to shrunken and damaged grains (Supplementary Fig. S5), and hence a significant loss of grain yield consistent with previous studies (Stone and Nicolas, 1996, 1998; Spiertz *et al.*, 2006; Prasad and Djanaguiraman, 2014).

Observed HS damage to grain yield was higher in tillers than in the main shoot (Fig. 6c, d) due to high senstivity of wheat at heading and anthesis stages (Prasad and Djanaguiraman, 2014). When HS was applied, the main shoots may have been past anthesis while tillers were in the heading or anthesis stages, and thus more exposed to HS impacts (Prasad and Djanaguiraman, 2014). FACE studies (Fitzgerald *et al.*, 2016; Macabuhay *et al.*, 2018) in wheat involving interactive effects eCO_2 and HS found that eCO_2 can buffer against heat waves, and eCO_2 may moderate some effects of HS in wheat depending on seasonal conditions and HS timing.

In conclusion, eCO_2 stimulated photosynthesis, biomass, and grain yield in a modern, high-yielding wheat variety. In non-HS plants, photosynthetic stimulation by eCO_2 was observed despite reduction of V_{cmax} at all temperatures and J_{max} at higher temperatures. In heat-shocked plants, eCO_2 stimulated J_{max} and maintained photochemical efficiency, hence providing photosynthetic protection against HS damage. Consequently, HS reduced photosynthesis under aCO_2 more than under eCO_2. Plant biomass completely recovered from HS under both CO_2 treatments due to the development of additional late tillers and ears; yet these did not fully develop and fill grains. Therefore, HS applied at anthesis equally reduced grain yield under aCO_2 and eCO_2 due to grain abortion. In the field, late tillers would not necessarily produce higher grain yield either, because plants will run out of soil water and there is not enough time for grain filling. The current study demonstrates the interactive impacts of eCO_2 and severe HS applied at 50% anthesis on wheat yield. HS can occur over a wide window from booting to late grain-filling stage, thus affecting yield in variable ways and limiting the generalization of our results. Nonetheless, our study provides insights into the interactive effects of eCO_2 and HS on the thermal responses of wheat photosynthesis which apply over a wide range of scenarios, and hence can form the basis for crop models to incorporate the interactive effects of eCO_2 and HS.

Supplementary data

Supplementary data are available at *JXB* online.

Table S1. Response of leaf gas exchange parameters to elevated CO_2 and heat stress.

Table S2. Response of plant dry mass and morphological parameters to elevated CO_2 and heat stress.

Table S3. Temperature response of mesophyll conductance in Scout.

Fig. S1. Glasshouse growth conditions and heat stress cycle.

Fig. S2. Radiation over time during the experiment.

Fig. S3. Experimental design depicting plant growth plotted over time.

Fig. S4. Temperature response of spot gas exchange parameters.

Fig. S5. Response of grain size and morphology to heat stress.

Acknowledgements

We thank Dr Craig Barton for support with leaf temperature measurements using thermocouples, and Ms Fiona Koller for assistance with biochemical assays. SGC was supported by the 'Agriculture, Fisheries & Forestry Postgraduate Research Scholarship' and Western Sydney University. The research received funding support by the Australian Commonwealth Department for Agriculture and Water Resources through the 'Filling the research gap' and was associated with the Australian Grains Free Air CO_2 Enrichment (AGFACE) programme run jointly by The University of Melbourne and Agriculture Research Victoria.

References

Ainsworth EA, Rogers A. 2007. The response of photosynthesis and stomatal conductance to rising [CO_2]: mechanisms and environmental interactions. Plant, Cell & Environment **30**, 258–270.

Alonso A, Pérez P, Martínez-Carrasco R. 2009. Growth in elevated CO_2 enhances temperature response of photosynthesis in wheat. Physiologia Plantarum **135**, 109–120.

Alonso A, Pérez P, Morcuende R, Martinez-Carrasco R. 2008. Future CO_2 concentrations, though not warmer temperatures, enhance wheat photosynthesis temperature responses. Physiologia Plantarum **132**, 102–112.

Amthor JS. 2001. Effects of atmospheric CO_2 concentration on wheat yield: review of results from experiments using various approaches to control CO_2 concentration. Field Crops Research **73**, 1–34.

Asseng S, Ewert F, Martre P, *et al*. 2015. Rising temperatures reduce global wheat production. Nature Climate Change **5**, 143–147.

Baker NR. 2008. Chlorophyll fluorescence: a probe of photosynthesis in vivo. Annual Review of Plant Biology **59**, 89–113.

Bányai J, Karsai I, Balla K, Kiss T, Bedő Z, Láng L. 2014. Heat stress response of wheat cultivars with different ecological adaptation. Cereal Research Communications **42**, 413–425.

Berry J, Bjorkman O. 1980. Photosynthetic response and adaptation to temperature in higher plants. Annual Review of Plant Physiology **31**, 491–543.

Borjigidai A, Hikosaka K, Hirose T, Hasegawa T, Okada M, Kobayashi K. 2006. Seasonal changes in temperature dependence of photosynthetic rate in rice under a free-air CO_2 enrichment. Annals of Botany **97**, 549–557.

Cai C, Yin X, He S, *et al*. 2016. Responses of wheat and rice to factorial combinations of ambient and elevated CO_2 and temperature in FACE experiments. Global Change Biology **22**, 856–874.

Coleman JS, Rochefort L, Bazzaz FA, Woodward FI. 1991. Atmospheric CO_2, plant nitrogen status and the susceptibility of plants to an acute increase in temperature. Plant, Cell & Environment **14**, 667–674.

Condon AG, Richards RA, Rebetzke GJ, Farquhar GD. 2004. Breeding for high water-use efficiency. Journal of Experimental Botany **55**, 2447–2460.

Crous KY, Quentin AG, Lin Y-S, Medlyn BE, Williams DG, Barton CVM, Ellsworth DS. 2013. Photosynthesis of temperate *Eucalyptus globulus* trees outside their native range has limited adjustment to elevated CO_2 and climate warming. Global Change Biology **19**, 3790–3807.

Delgado E, Mitchell RAC, Parry MAJ, Driscoll SP, Mitchell VJ, Lawlor DW. 1994. Interacting effects of CO_2 concentration, temperature and nitrogen supply on the photosynthesis and composition of winter wheat leaves. Plant, Cell & Environment **17**, 1205–1213.

Dias de Oliveira EA, Siddique KHM, Bramley H, Stefanova K, Palta JA. 2015. Response of wheat restricted-tillering and vigorous growth traits to variables of climate change. Global Change Biology **21**, 857–873.

Dreccer MF, Wockner KB, Palta JA, McIntyre CL, Borgognone MG, Bourgault M, Reynolds M, Miralles DJ. 2014. More fertile florets and grains per spike can be achieved at higher temperature in wheat lines with high spike biomass and sugar content at booting. Functional Plant Biology **41**, 482–495.

Duursma RA. 2015. Plantecophys—an R package for analysing and modelling leaf gas exchange data. PLoS One **10**, e0143346.

Eckardt NA, Portis AR. 1997. Heat denaturation profiles of ribulose-1,5-bisphosphate carboxylase/oxygenase (Rubisco) and Rubisco activase and the inability of Rubisco activase to restore activity of heat-denatured Rubisco. Plant Physiology **113**, 243–248.

Evans J, Sharkey T, Berry J, Farquhar G. 1986. Carbon isotope discrimination measured concurrently with gas exchange to investigate CO_2 diffusion in leaves of higher plants. Functional Plant Biology **13**, 281–292.

Evans JR, Von Caemmerer S. 2013. Temperature response of carbon isotope discrimination and mesophyll conductance in tobacco. Plant, Cell & Environment **36**, 745–756.

FAO. 2019. http://www.fao.org/faostat/en/#data/QC accessed on 16 May 2019.

Farooq M, Bramley H, Palta JA, Siddique KHM. 2011. Heat stress in wheat during reproductive and grain-filling phases. Critical Reviews in Plant Sciences **30**, 491–507.

Farquhar GD, Cernusak LA. 2012. Ternary effects on the gas exchange of isotopologues of carbon dioxide. Plant, Cell & Environment **35**, 1221–1231.

Fitzgerald GJ, Tausz M, O'Leary G, *et al*. 2016. Elevated atmospheric [CO_2] can dramatically increase wheat yields in semi-arid environments and buffer against heat waves. Global Change Biology **22**, 2269–2284.

Ghannoum O, Phillips NG, Sears MA, Logan BA, Lewis JD, Conroy JP, Tissue DT. 2010. Photosynthetic responses of two eucalypts to industrial-age changes in atmospheric [CO_2] and temperature. Plant, Cell & Environment **33**, 1671–1681.

Haque MS, Kjaer KH, Rosenqvist E, Sharma DK, Ottosen C-O. 2014. Heat stress and recovery of photosystem II efficiency in wheat (*Triticum aestivum* L.) cultivars acclimated to different growth temperatures. Environmental and Experimental Botany **99**, 1–8.

Harley PC, Thomas RB, Reynolds JF, Strain BR. 1992. Modelling photosynthesis of cotton grown in elevated CO_2. Plant, Cell & Environment **15**, 271–282.

Hikosaka K, Ishikawa K, Borjigidai A, Muller O, Onoda Y. 2006. Temperature acclimation of photosynthesis: mechanisms involved in the changes in temperature dependence of photosynthetic rate. Journal of Experimental Botany **57**, 291–302.

Hocking PJ, Meyer CP. 1991. Effects of CO_2 enrichment and nitrogen stress on growth and partitioning of dry matter and nitrogen in wheat and maize. Australian Journal of Plant Physiology **18**, 339–356.

Hogan KP, Smith AP, Ziska LH. 1991. Potential effects of elevated CO_2 and changes in temperature on tropical plants. Plant, Cell & Environment **14**, 763–778.

Hunsaker DJ, Kimball BA, Pinter PJ Jr, Wall GW, LaMorte RL, Adamsen FJ, Leavitt SW, Thompson TL, Matthias AD, Brooks TJ. 2000. CO_2 enrichment and soil nitrogen effects on wheat evapotranspiration and water use efficiency. Agricultural and Forest Meteorology **104**, 85–105.

Hunsaker DJ, Kimball BA, Pinter PJ, LaMorte RL, Wall GW. 1996. Carbon dioxide enrichment and irrigation effects on wheat evapotranspiration and water use efficiency. Transactions of the ASAE **39**, 1345–1355.

Jauregui I, Aroca R, Garnica M, Zamarreño ÁM, García-Mina JM, Serret MD, Parry M, Irigoyen JJ, Aranjuelo I. 2015. Nitrogen assimilation and transpiration: key processes conditioning responsiveness of wheat to elevated [CO_2] and temperature. Physiologia Plantarum **155**, 338–354.

Kimball BA. 1983. Carbon dioxide and agricultural yield: an assemblage and analysis of 430 prior observations. Agronomy Journal **75**, 779–788.

Kimball BA, LaMorte RL, Pinter PJ, Wall GW, Hunsaker DJ, Adamsen FJ, Leavitt SW, Thompson TL, Matthias AD, Brooks TJ. 1999. Free-air CO_2 enrichment and soil nitrogen effects on energy balance and evapotranspiration of wheat. Water Resources Research **35**, 1179–1190.

Kimball BA, Pinter PJ Jr, Garcia RL, La Morte RL, Wall GW, Hunsaker DJ, Wechsung G, Wechsung F, Kartschall T. 1995. Productivity and water use of wheat under free-air CO_2 enrichment. Global Change Biology **1**, 429–442.

Lanigan GJ, Betson N, Griffiths H, Seibt U. 2008. Carbon isotope fractionation during photorespiration and carboxylation in *Senecio*. Plant Physiology **148**, 2013–2020.

Leakey ADB, Ainsworth EA, Bernacchi CJ, Rogers A, Long SP, Ort DR. 2009. Elevated CO_2 effects on plant carbon, nitrogen, and water relations: six important lessons from FACE. Journal of Experimental Botany **60**, 2859–2876.

Lobell DB, Gourdji SM. 2012. The influence of climate change on global crop productivity. Plant Physiology **160**, 1686–1697.

Lobell DB, Schlenker W, Costa-Roberts J. 2011. Climate trends and global crop production since 1980. Science **333**, 616–620.

Long SP. 1991. Modification of the response of photosynthetic productivity to rising temperature by atmospheric CO_2 concentrations: has its importance been underestimated? Plant, Cell & Environment **14**, 729–739.

Macabuhay A, Houshmandfar A, Nuttall J, Fitzgerald GJ, Tausz M, Tausz-Posch S. 2018. Can elevated CO_2 buffer the effects of heat waves on wheat in a dryland cropping system? Environmental and Experimental Botany **155**, 578–588.

Medlyn BE, Dreyer E, Ellsworth D, *et al*. 2002. Temperature response of parameters of a biochemically based model of photosynthesis. II. A review of experimental data. Plant, Cell & Environment **25**, 1167–1179.

Miglietta F, Giuntoli A, Bindi M. 1996. The effect of free air carbon dioxide enrichment (FACE) and soil nitrogen availability on the photosynthetic capacity of wheat. Photosynthesis Research **47**, 281–290.

Morison JIL. 1998. Stomatal response to increased CO_2 concentration. Journal of Experimental Botany **49**, 443–452.

Morison JIL, Lawlor DW. 1999. Interactions between increasing CO_2 concentration and temperature on plant growth. Plant, Cell & Environment **22**, 659–682.

Nie GY, Long SP, Garcia RL, Kimball BA, Lamorte RL, Pinter PJ, Wall GW, Webber AN. 1995. Effects of free-air CO_2 enrichment on the development of the photosynthetic apparatus in wheat, as indicated by changes in leaf proteins. Plant, Cell & Environment **18**, 855–864.

Osborne CP, Roche JL, Garcia RL, Kimball BA, Wall GW, Pinter PJ, Morte RL, Hendrey GR, Long SP. 1998. Does leaf position within a canopy affect acclimation of photosynthesis to elevated CO_2? Analysis of a wheat crop under free-air CO_2 enrichment. Plant Physiology **117**, 1037–1045.

Pan C, Ahammed GJ, Li X, Shi K. 2018. Elevated CO_2 improves photosynthesis under high temperature by attenuating the functional limitations to energy fluxes, electron transport and redox homeostasis in tomato leaves. Frontiers in Plant Science **9**, 1739.

Paul MJ, Foyer CH. 2001. Sink regulation of photosynthesis. Journal of Experimental Botany **52**, 1383–1400.

Perdomo JA, Capó-Bauçà S, Carmo-Silva E, Galmés J. 2017. Rubisco and Rubisco activase play an important role in the biochemical limitations of photosynthesis in rice, wheat, and maize under high temperature and water deficit. Frontiers in Plant Science **8**, 490.

Prasad PVV, Djanaguiraman M. 2014. Response of floret fertility and individual grain weight of wheat to high temperature stress: sensitive stages and thresholds for temperature and duration. Functional Plant Biology **41**, 1261–1269.

Rawson H. 1992. Plant responses to temperature under conditions of elevated CO_2. Australian Journal of Botany **40**, 473–490.

R Core Team. 2017. R: a language and environment for statistical computing. Vienna, Austria: R Foundation for Statistical Computing.

Sage RF, Kubien DS. 2007. The temperature response of C3 and C4 photosynthesis. Plant, Cell & Environment **30**, 1086–1106.

Shanmugam S, Kjaer KH, Ottosen C-O, Rosenqvist E, Kumari Sharma D, Wollenweber B. 2013. The alleviating effect of elevated CO_2 on heat stress susceptibility of two wheat (*Triticum aestivum* L.) cultivars. Journal of Agronomy and Crop Science **199**, 340–350.

Sharkova VE. 2001. The effect of heat shock on the capacity of wheat plants to restore their photosynthetic electron transport after photoinhibition or repeated heating. Russian Journal of Plant Physiology **48**, 793–797.

Sharma DK, Andersen SB, Ottosen C-O, Rosenqvist E. 2014. Wheat cultivars selected for high F_v/F_m under heat stress maintain high photosynthesis, total chlorophyll, stomatal conductance, transpiration and dry matter. Physiologia Plantarum **153**, 284–298.

Sharwood RE, von Caemmerer S, Maliga P, Whitney SM. 2008. The catalytic properties of hybrid Rubisco comprising tobacco small and sunflower large subunits mirror the kinetically equivalent source Rubiscos and can support tobacco growth. Plant Physiology **146**, 83–96.

Silva-Pérez V, Furbank RT, Condon AG, Evans JR. 2017. Biochemical model of C3 photosynthesis applied to wheat at different temperatures. Plant, Cell & Environment **40**, 1552–1564.

Singsaas EL, Ort DR, Delucia EH. 2004. Elevated CO_2 effects on mesophyll conductance and its consequences for interpreting photosynthetic physiology. Plant, Cell & Environment **27**, 41–50.

Spiertz JHJ, Hamer RJ, Xu H, Primo-Martin C, Don C, van der Putten PEL. 2006. Heat stress in wheat (*Triticum aestivum* L.): effects on grain growth and quality traits. European Journal of Agronomy **25**, 89–95.

Stone PJ, Nicolas M. 1996. Effect of timing of heat stress during grain filling on two wheat varieties differing in heat tolerance. II. Fractional protein accumulation. Functional Plant Biology **23**, 739–749.

Stone PJ, Nicolas ME. 1994. Wheat cultivars vary widely in their responses of grain yield and quality to short periods of post-anthesis heat stress. Functional Plant Biology **21**, 887–900.

Stone PJ, Nicolas ME. 1998. The effect of duration of heat stress during grain filling on two wheat varieties differing in heat tolerance: grain growth and fractional protein accumulation. Functional Plant Biology **25**, 13–20.

Wahid A, Gelani S, Ashraf M, Foolad MR. 2007. Heat tolerance in plants: an overview. Environmental and Experimental Botany **61**, 199–223.

Walker AP, Beckerman AP, Gu L, Kattge J, Cernusak LA, Domingues TF, Scales JC, Wohlfahrt G, Wullschleger SD, Woodward FI. 2014. The relationship of leaf photosynthetic traits—V_{cmax} and J_{max}—to leaf nitrogen, leaf phosphorus, and specific leaf area: a meta-analysis and modeling study. Ecology and Evolution **4**, 3218–3235.

Wang D, Heckathorn SA, Barua D, Joshi P, Hamilton EW, LaCroix JJ. 2008. Effects of elevated CO_2 on the tolerance of photosynthesis to acute heat stress in C3, C4, and CAM species. American Journal of Botany **95**, 165–176.

Wang D, Heckathorn SA, Wang X, Philpott SM. 2011. A meta-analysis of plant physiological and growth responses to temperature and elevated CO_2. Oecologia **169**, 1–13.

Yamasaki T, Yamakawa T, Yamane Y, Koike H, Satoh K, Katoh S. 2002. Temperature acclimation of photosynthesis and related changes in photosystem II electron transport in winter wheat. Plant Physiology **128**, 1087–1097.

Zhang X, Högy P, Wu X, Schmid I, Wang X, Schulze WX, Jiang D, Fangmeier A. 2018. Physiological and proteomic evidence for the interactive effects of post-anthesis heat stress and elevated CO_2 on wheat. Proteomics **18**, 1800262.

Zinta G, AbdElgawad H, Domagalska MA, Vergauwen L, Knapen D, Nijs I, Janssens IA, Beemster GTS, Asard H. 2014. Physiological, biochemical, and genome-wide transcriptional analysis reveals that elevated CO_2 mitigates the impact of combined heat wave and drought stress in *Arabidopsis thaliana* at multiple organizational levels. Global Change Biology **20**, 3670–3685.